Decoding Efficiency Optimization in an Asynchronous NOMA-assisted D2D Network

***Abstract*—Nowadays, massive device-to-device (D2D) networks are in demand due to their key merits namely i) infrastructure-free network, ii) ability to operate with limited resources and iii) ubiquitous connectivity to the end-users. However, the overall performance of the D2D network merely degrades due to the complex decoding procedure followed by the user terminals. In this paper, an asynchronous NOMA (A-NOMA)-based cyclic triangular successive interference cancellation (Cyclic T-SIC) scheme is proposed to optimize the decoding efficiency at the receiver terminals of a D2D network. In particular, the Cyclic T-SIC scheme follows three processes: i) optimization process ii) decoding process and iii) re-transmission process. In the first process, a dual Lagrangian objective function is defined to select the best combination of data symbols to be decoded at the receiver terminal, under statistical interference threshold and data rate constraints. Then, in the second process, the selected data symbols in the optimization process will be decoded using the triangular SIC (T-SIC) method. Next, in the third process, the receiver has to wait for the retransmissions from the rest of the users whose data has not yet been decoded correctly. The Cyclic T-SIC scheme will remain active until the last user's data in the superimposed signal is decoded correctly. The performance metrics of the proposed Cyclic T-SIC scheme are defined in terms of energy efficiency, bit error rate, computational complexity, and decoding delay parameters. Furthermore, numerical results of the network are obtained and compared with the conventional T-SIC by varying the number of users, received power ratio, and transmit signal-to-noise ratio (SNR). The validation of the obtained results is done through computer simulation analysis.**

***Index Terms*—Asynchronous NOMA, Device-to-device network, Energy efficiency, Optimization, Cyclic T-SIC, Successive interference cancellation**

I. Introduction

The forthcoming beyond-5G/6G network is expected to provide reliable, error-free, and energy-efficient services with ubiquitous connectivity [1]. On the other hand, the usage of new wireless devices is also increasing the mobile traffic by thousand times in comparison to the existing networking systems [2]. In this context, widely used 5G orthogonal multiple access (OMA) schemes such as orthogonal frequency division multiple access (OFDMA) [3] and code division multiple access (CDMA) [4] can support a large number of devices by utilizing the existing network resources effectively. In particular, the CDMA scheme diversifies the users based on the unique spreading sequences allocated for data transmission but such spreading sequences may not be sufficient to cater to a large number of users. Moreover, in OFDMA, the complete bandwidth of the channel is allocated to all the sub-carriers in such a manner that the interference between each sub-carriers can be minimized. Since the number of sub-carriers within the bandwidth is limited, there arises a spectral availability limitation in the existing D2D wireless networks.

In comparison to OMA schemes, the non-orthogonal multiple access (NOMA) scheme is an emerging technology that has the potential to enhance the spectral efficiency of the D2D network by allowing multiple users to simultaneously access the same resource blocks (RBs) [5]. The fundamental concept of NOMA is based on superposition coding and successive decoding where the superposition coding of multiple users' signals can be done over the same subcarrier with different power levels that enables the receiver to decode the signal by using the successive interference cancellation (SIC) technique [6]. At the receiver, the SIC starts by decoding the data of the user having the strongest signal-to-noise ratio (SNR) up to the last user in descending order of SNRs. Once the strongest signal is directly decoded, the detected data is passed through to an iterative SIC algorithm. Next, the strongest signal is reconstructed based on the prior known knowledge of channel state information (CSI) and the modulation scheme used for transmission. Then, the reconstructed signal is subtracted from the received superimposed symbol to reduce its interference and increase accuracy in decoding the rest of the user data signals. Indeed, such a SIC decoding scheme is applicable for time-synchronous transmissions.

In practice, time-synchronous data reception is not possible at the receiver terminals in the D2D networks since the transmitting users are geographically distributed and signals from different transmitters propagate via different paths and encounter different channel effects [7], [8]. These result in different time offsets when signals from different users arrive at a receiving device. Hence, authors in [9] have proposed a novel asynchronous SIC method named triangular SIC (T-SIC) decoding for uplink NOMA transmissions. This scheme enables decoding user data considering time offset among received signals due to the difference in propagation paths and channel effects. Hence, time offset among different users causes symbols of such users to overlap with the other users. Hence, the interference from overlapping symbols must be considered in asynchronous NOMA (A-NOMA) during the decoding of the desired user data. [9] has shown that the T-SIC technique with iterative signal processing provides an enhanced BER and spectral efficiency performance compared to the conventional SIC decoding in uplink A-NOMA transmissions. In conventional SIC, the interference from the overlapping symbols due to the asynchrony in transmissions is neglected and hence does not completely cancel out the interference from overlapping symbols. Such phenomena reduce

the probability of correct symbol detection and hence increase the BER. Further, the throughput is reduced in the conventional SIC scheme because of neglecting the added interference due to the overlapping symbols.

In addition, studies on uplink A-NOMA schemes have shown improved BER and throughput performance than conventional synchronized uplink NOMA schemes [9]–[13]. In [14], an uplink A-NOMA scheme with equal-power asynchronous transmissions is discussed, where it is proven that the asynchrony in the transmission actually enhance the signal detection. Moreover, the optimal mismatch between user signals in an uplink A-NOMA for enhanced throughput and energy efficiency is analytically presented in [15]. Further, it is claimed in [16] that the optimal SIC decoding in A-NOMA depend upon the users' channel strengths. Moreover, authors in [10] have proposed and experimentally implemented an A-NOMA scheme for an uplink optical access scenario, which has a higher BER reduction of one order magnitude than the conventional synchronous NOMA schemes. Moreover, in [12], an uplink A-NOMA with a sufficiently large data frame length has been shown to out perform synchronous NOMA in terms of sum throughput. Additionally, in [13], the impact of synchronization and coordination timing errors on uplink A-NOMA is investigated. The synchronization timing error has been shown to have a higher impact on throughput compared to the coordination error [13].

In addition to improving spectral efficiency and reliability, one of the main targets of future 6G networks is maximizing energy efficiency (EE) [1], [17], [18]. Massive NOMA communication systems conventionally suffer from high complexity during the decoding phase where the SIC method is used [19], [20]. The authors in [21] claim the increase in complexity during NOMA decoding when the number of users increase for more than three. Increment in complexity can lead to higher energy consumption and hence reduced energy efficiency. Furthermore, energy consumption at mobile devices can be higher, particularly in energy limited scenarios such as emergency disaster scenarios, since such devices cannot cope flexibly with energy consuming computations [22], [23]. Further, issues such as limited resources for allocation, complex SIC decoding procedure in massive asynchronous transmissions, can be observed in NOMA based out-band asynchronous D2D. It was noted that, a reliable and an efficient A-NOMA for outband D2D networks was understudied. Thus, decoding efficiency optimization algorithm that maximizes the number of data symbols decoded under signal power and interference-noise power constraints is required for NOMA-based asynchronous D2D communications. Therefore, the objective of this paper is to investigate and optimize the performance of massive A-NOMA D2D transmissions. The main contributions of this work can be summarized as follows:

- Performance in an A-NOMA assisted massive D2D communications is studied in this work. In such a scenario, a superimposed signal with multiple data signals is received at the receiver end terminal. Decoding of such a large superimposed signal consume a higher computational cost due to the complexity in the A-NOMA decoding procedure. A novel optimization algorithm is proposed to decide the optimal combination of data symbols in the superimposed signal to be decoded per iteration under maximum interference power and minimum rate constraints.
- In order to select the best combination of data symbols, constraints of the the optimization problem is considered taking into account the energy consumption for interference cancellation and decoding reliability of such data. The optimal selection of data symbols will be given as a binary variable and hence will be non-convex. Further, the minimum rate constraint will be a non linear constraint. Hence, such binary and non linear constraints are reformulated as continuous and linear constraints and the equivalent Lagrangian dual objective function is formed so that it can be solved efficiently by applying the Lagrangian dual algorithm.
- A novel scheme called Cyclic T-SIC is proposed, to ensure decoding each users' data in multiple iterations, considering also the retransmissions by the users whose data were not yet decoded in the first iteration of optimization. Hence, the process of listening to the same subcarrier, receiving the remaining users' data, and decoding based on the optimization output will be continued at the receiver UE, until each users' data have been decoded. Moreover, the EE and BER performance of the Cyclic T-SIC is presented under the impact of number of users, received power ratio (ν), transmit SNR, and compared with *Conv T-SIC*.
- The optimal trade-off between the BER and EE of the proposed Cyclic T-SIC is studied, under varying parameters such as ν, transmit SNR, and relative symbol time offset and compared with *Conv T-SIC*. The optimal point that can achieve a higher EE and reduced BER shows that the proposed Cyclic T-SIC can achieve such a point with lower transmit SNR, ν compared to *Conv T-SIC*. Further, it was found that a lower BER and higher EE can be obtained, even if the relative symbol time-offset increases the asynchrony among the received data signals, using the proposed Cyclic T-SIC scheme.
- The computational complexity of the proposed Cyclic T-SIC over n iterations is proven to be less than that of the *Conv T-SIC* scheme when the error tolerance for algorithm termination, ϵ, is in the order of 10^{-1} magnitude. Further, the total simulation delay is shown to be lesser in Cyclic T-SIC than *Conv T-SIC* due to its reduced computational complexity.

The remaining of this paper is organized as follows. In Section II, the signal model and schemes are introduced, including the received signal structure and the iterative signal processing at the receiver. Section III presents the problem formulation and the proposed Cyclic T-SIC scheme is presented in Section IV. Next, the performance analysis is given in Section IV. Furthermore, a result analysis is presented in Section VI.

Finally, conclusions are drawn with remarks in Section VII.

II. Asynchronous signal model and schemes

In this Section, an uplink A-NOMA signal model, its preliminaries and existing A-NOMA T-SIC schemes are presented.

A. Signal model

An A-NOMA assisted D2D network with $k \in K$ geographically distributed transmitting UEs and one receiving UE, R, within a small neighborhood is considered as shown in Figure. 1. It is assumed that there are N subcarriers and each subcarrier is shared by K users, $K \geq 1$.

B. System preliminaries

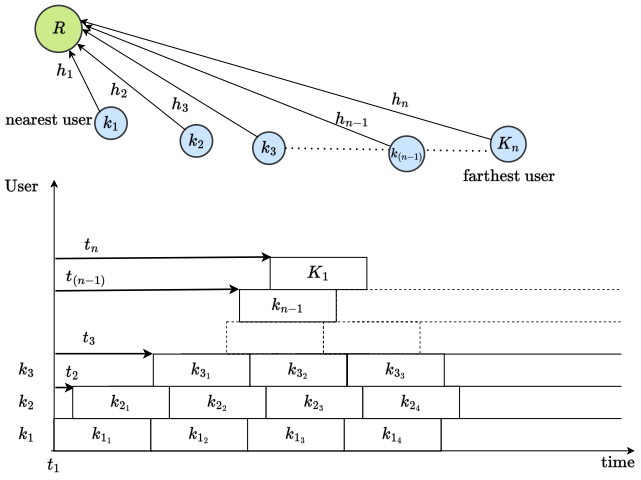

Figure 1: A-NOMA assisted D2D communication with a K number of transmitters and one receiving UE.

The received signal at R for the k^*th user at the sth symbol is given by,

$$Y_{k^*}[s] = h_{k^*}\sqrt{P_{k^*}}X_{k^*}[s] + \eta_{k^*}[s] + n_0, \tag{1}$$

where $X_{k^*}[s]$ denote the sth symbol of the k^*th user's data which is a complex symbol and output from a multi level symbol mapper such as quadrature amplitude modulation (QAM).

Moreover, P_{k^*} is the transmit power of $X_{k^*}[s]$, which is same for all symbols of k^*th user for the transmission time duration. Hence, the signal transmitted from the k^*th user at the sth symbol can be represented by $\sqrt{P_{k^*}}X_{k^*}[s]$. For one symbol time period, the frequency response on one subcarrier was considered flat and was assumed to follow a Rayleigh distribution independently and identically (i.i.d). The channel coherence time is assumed to be much larger than the symbol time and hence $h_{k^*}[s]$ is fixed for a block of symbols during a transmission period. Hence, channel, h_{k^*}, is considered constant throughout the subcarrier time period and it is used to denote the channel state information (CSI). Further, n_0 is the additive white Gaussian noise (AWGN) at the receiver side with variance σ^2 and $\eta_{k^*}[s]$ is the total interference to the desired symbol sth symbol of k^*th user.

$$\eta_{k^*}[s] = \sum_{i\neq k^*}^{K}\sum_{\varsigma=s-1}^{s+1}\Delta_{k^*,i}[s,\varsigma]X_i[s].h_i\sqrt{P_i}.e^{j\theta_{k^*,i}}, \tag{2}$$

where $e^{j\theta_{k^*,i}}$ represents the phase mismatch of the i^{th} user's signal to the k^*th and $\Delta_{k^*,i}$ represents the percentage of symbol duration that the ς symbol of the i^{th} user overlap with the desired symbol out of the total symbol period, T_{sym}.

Following the standard SIC procedure, after subtracting the reconstructed interference, $\hat{\eta}_{k^*,i}[s,\varsigma]$, of all overlapping symbols of interferes, the interference cancelled (ICed) signal for desired symbol can be expressed in terms of desired signal and residual interference plus noise as,

$$\begin{aligned} Y_{k^*}[s] &= Y_{k^*}[s] - \sum_{i\neq k^*}^{K}\sum_{\varsigma=s-1}^{s+1}\hat{\eta}_{k^*,i}[s,\varsigma], \\ &= X_{k^*}[s].h_i\sqrt{P_i}.e^{j\theta_{k^*,i}} + \tilde{\eta}_{k^*}[s] + n_0, \end{aligned} \tag{3}$$

where the latest residual interference to the desired symbol, k^*, can be modelled as,

$$\tilde{\eta}_{k^*}[s] = \sum_{i\neq k^*}^{K}\sum_{\varsigma=s-1}^{s+1}\Delta_{k^*,i}[s,\varsigma](X_i[s] - \hat{X}_i[s]).h_i\sqrt{P_i}.e^{j\theta_{k^*,i}}, \tag{4}$$

Moreover, by considering the latest detected symbols, the signal to noise ratio (SINR) of the sth symbol of the k^*th user can be expressed with respect to $\tilde{\eta}_{k^*}[s]$ as,

$$(\gamma_{k^*}[s]|\mathbf{z}, h_{k^*}, \Delta_{k^*}) = \frac{P_{k^*}g_{k^*}}{\mathrm{Var}(\tilde{\eta}_{k^*}[s]|\mathbf{z}, h_{k^*}, \Delta_{k^*}) + \sigma^2}, \tag{5}$$

where $\mathbf{z}$ represent the latest detection status of the interfering symbols, i.e. correct or erroneous.

C. Existing A-NOMA vs conventional NOMA SIC decoding

In synchronous NOMA, the received superimposed data signal from multiple transmitters is assumed to be time synchronized. The main difference in A-NOMA compared to synchronous NOMA is that the symbols in a subcarrier from the different users are time misaligned such that it causes the desired user's symbol to overlap with one or more symbols of each of the interfering users. The synchronous SIC scheme decodes data from only a single symbol of each user, whereas the asynchronous SIC scheme requires information from multiple symbols to decode the desired user's symbol. Moreover, the authors in [9], have proposed a SIC decoding method for NOMA based asynchronous transmissions called T-SIC.

D. T-SIC decoding scheme

The procedure followed in triangular SIC (T-SIC) scheme in [9] is as follows. First, an IC triangle is constructed by exploiting the triangular pattern of detection of data symbols. The triangular pattern starts to form the IC triangle with the

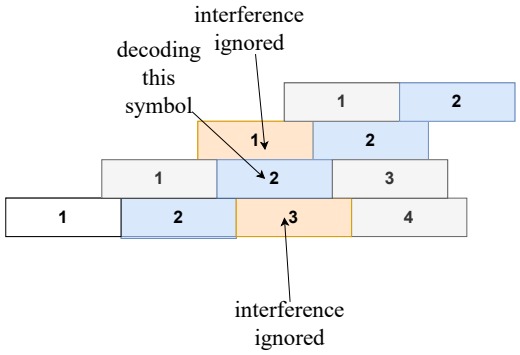

Figure 2: Drawback of Conventional SIC decoding

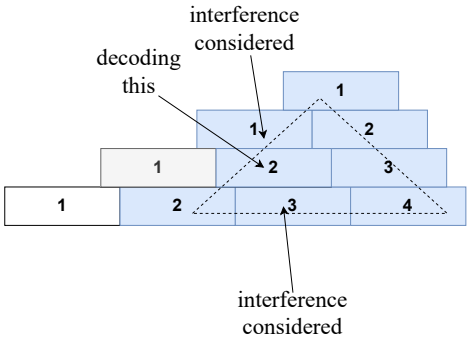

Figure 3: Advantage of Triangle SIC decoding in [9]

weakest symbol received and sets it as the last symbol to be detected. Next, the symbols that overlap with weakest user's symbol are added to the IC triangle. Then, all the symbols that overlap the second weakest users' symbols are included to the IC triangle. This procedure is repeated until the strongest users' symbols are added to the IC triangle. Hence, finally a triangle is formed as given in Fig. 4.

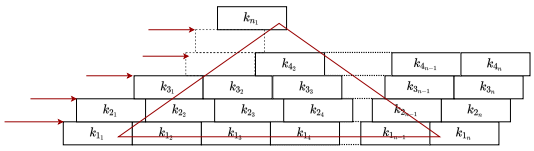

Figure 4: Procedure of Triangle SIC decoding in [9]

Once a superimposed data signal y is received, the first symbol of k_1 is decoded. Next the consecutive symbols of k_1 are decoded. Afterwards, the first symbol of k_2 are decoded by subtraction of prior estimated symbols. Then, the first symbol of the k_2 user is decoded by subtracting the prior estimated symbols belonging to k_1. The second symbol of k_2 user is decoded by subtracting all the prior estimated symbols that belong to both k_1, k_2 from the received signal y. Similarly, the symbols of k_3, up to k_n users are decoded by subtracting the prior symbols estimated. Further, Fig. 4 illustrates the iterative SIC decoding structure of conventional Triangular SIC (T-SIC). In the forthcoming section, a decoding efficiency optimization algorithm for asynchronous SIC decoding to improve decoding efficiency in terms of factors such as energy consumption, reliability, complexity, delay is proposed.

III. Problem Formulation

In order to resolve the decoding efficiency in D2D A-NOMA, an optimization algorithm is proposed to decide the optimal combination of data symbols decoded per iteration at a receiver UE, that receives a superimposed NOMA signal. The goal is to reduce the complexity of decoding per iteration. Hence, the optimization problem can be formulated as follows.

$$\underset{D_{u_k}}{\text{maximize}} \quad \sum_{k=1}^{K} D_{u_k}.(K-k+1) \tag{6a}$$

$$\text{subject to} \quad D_{u_k} \in \{0,1\}, \forall k \in K, \tag{6b}$$

$$D_{u_{(k+1)}} - D_{u_k} \leq 0, \tag{6c}$$

$$D_{u_k}.(B.log_2(1+\sum_{s=1}^{K-k+1} \gamma_k[s]) - R_{\min}) \geq 0, \tag{6d}$$

$$0 \leq \sum_{k=1}^{K} D_{u_k} \sum_{i \neq k}^{K} \sum_{\varsigma=s-1}^{s+1} \Delta_{k,i}[s,\varsigma] \leq \frac{I_{th}}{t_{ts}}, \tag{6e}$$

where $D_{u_k}, \Delta_i, I_{th}, t_{ts}$, represent respectively, the decision of user data selected, the duration of symbol time that i^{th} user overlap with the desired k^{th} user symbol, statistical interference power threshold per T-SIC iteration, unit time slot duration. The optimal number of user data, k_{opt}, that will be decoded per single SIC iteration is given by,

$$k_{\text{opt}} = \sum_{k=1}^{K} D_{u_k} \tag{7}$$

The solution of problem in (6a) is D_u, is a binary vector that select the range of user data selected. Hence, each k^{th} element of D_u is binary and the selected user data should be in the order of strongest user to the weakest user signal which is modelled as a constraint in (6c).

The constraint in (6d) corresponds to the minimum rate constraint for each data received. The constraint (6e) corresponds to the minimum allowable energy threshold per single SIC iteration. Note that constraint (6d) can be transformed as the following equivalent form where $\tilde{\gamma} = 2^{R_{\min}} - 1$.

$$D_{u_k}.(\sigma^2 + \sum_{i=1}^{K} \sum_{\varsigma=s-1}^{s+1} P_i g_i \Delta_{k,i}[s,\varsigma] - P_k g_k (1 + \frac{1}{\tilde{\gamma}})) \leq 0 \tag{8}$$

A. Binary constraint relaxation

Since the problem in (6a) is non-convex due to the binary and non linear constraints, the above problem is transformed into the following form, where the binary constraint in (6b) is transformed to linear constraints (9b), and (9c). Such constraint re-formulation can assure that the value of u_k is approximated to a binary. Further, the non linear constraint

with regard to *SINR* constraints in (6d) is converted into a linear constraint as in (8).

$$\begin{aligned} \underset{D_{u_k}}{\text{maximize}} \quad & \sum_{k=1}^{K} D_{u_k}.(K-k+1) && \text{(9a)} \\ \text{subject to} \quad & 0 \leq D_{u_k} \leq 1, \forall k \in K, && \text{(9b)} \\ & \sum_{k=1}^{K} (D_{u_k} - D_{u_k}^2) \leq 0, && \text{(9c)} \\ & D_{u_{(k+1)}} - D_{u_k} \leq 0, && \text{(9d)} \\ & (6e), (8), && \text{(9e)} \end{aligned}$$

where $P_k, g_k, \sigma^2, P_{th}, g_{th}, P_i, g_i,$ represent respectively, the transmission power of k^{th} user, channel gain of k^{th} user, thermal noise variance, threshold transmission power corresponding to *SINR*$_{\text{th}}$, channel gain corresponding to *SINR*$_{\text{th}}$, transmission power of i^{th} user, channel gain of i^{th} user. Since the constraint in (9c) is concave, the Lagrangian duality of such constraint can be considered as presented in [24], [25].

B. Lagrangian objective function

The Lagrangian objective function of problem (6a) is formed as,

$$\begin{aligned} \mathcal{L}(D_{u_k}, \lambda) = & -\sum_{k=1}^{K} D_{u_k}.(K-k+1) \\ & - \sum_{k=1}^{K} \lambda_k D_{u_k} + \sum_{k=1}^{K} \lambda_k D_{u_k}^2 \\ & - \sum_{k=1}^{K} v_k \Bigg(D_{u_k}.(\sigma^2 + \sum_{i=1}^{K} \sum_{\varsigma=s-1}^{s+1} P_i g_i \Delta_{k,i}[s,\varsigma] \\ & - P_k g_k (1 + \frac{1}{\tilde{\gamma}})) \Bigg) \\ & - \Bigg(\sum_{k=1}^{K} \mu_k.D_{u_k} \sum_{i \neq k}^{K} \sum_{\varsigma=s-1}^{s+1} \Delta_{k,i}[s,\varsigma] - \frac{I_{th}}{t_{ts}} \Bigg), \end{aligned} \tag{10}$$

where, $\lambda, \mathbf{v}, \mu$ are the Lagrangian multipliers corresponding respectively to binary constraint in (9c), minimum rate constraint in (8) and interference threshold constraint in (6e) .

C. Dual objective function

Further, the dual objective function is given by,

$$g(\lambda) = \max_{\{D_{u_k}\}} \mathcal{L}(D_{u_k}, \lambda). \tag{11}$$

and the dual optimization problem is formulated as follows

$$\begin{aligned} \underset{\lambda}{\text{minimize}} \quad & g(\lambda) && \text{(12a)} \\ \text{subject to} \quad & \lambda \succcurlyeq 0. && \text{(12b)} \end{aligned}$$

Note that the objective function as well as all the constraints of the dual problem are all linear with respect to Lagrangian multiplier. Thus, the dual problem is convex over dual variable μ, ς which can be optimized through a one dimensional searching algorithm.

D. Gradient descent algorithm

The optimal D_u can be achieved by running the problem in a CVX solver. However, in case where different feasible solutions are generated, the solution that is converging can be considered as the optimal solution. Hence, a gradient descent algorithm [26] can used to find such converging solution for D_u.

Hence, first the gradient of the Lagrangian function with respect to D_{u_k} which is formulated as follows.

$$\nabla_{D_{u_k}} \mathcal{L} = -(K-k+1) - \lambda + 2\lambda.D_{u_k}. \tag{13}$$

Further, D_{u_k} can be updated as follows,

$${D_{u_k}}^{(n)} = {D_{u_k}}^{(n-1)} + \beta.\nabla_{{D_{u_k}}^{n-1}} \mathcal{L}, \tag{14}$$

where β denotes the iteration step size of D_u. After finding the optimal D_u using gradient descent the optimal λ can be achieved.

The dual function in (12a) is not guaranteed to be differentiable. Hence, the sub gradient algorithm in [18] is used to formulate the iterative process to find the optimal λ.

An iterative scheme based on gradient descent algorithm is used to obtain the optimal λ. The sub-gradient of the dual function with respect to λ can be derived as

$$\nabla_\lambda \ g(\lambda) = -\sum_{k=1}^{K} D_{u_k} + \sum_{k=1}^{K} D_{u_k}^2. \tag{15}$$

Further, dual variable λ can be updated according to the following expression.

$$\lambda^{(m)} = \lambda^{(m-1)} + \alpha.\nabla_{\lambda^{m-1}} \tag{16}$$

where α denotes the iteration step size of λ. The approach to solve the optimization problem in (6a) is summarized in Algorithm 1.

IV. Sequential T-SIC decoding scheme

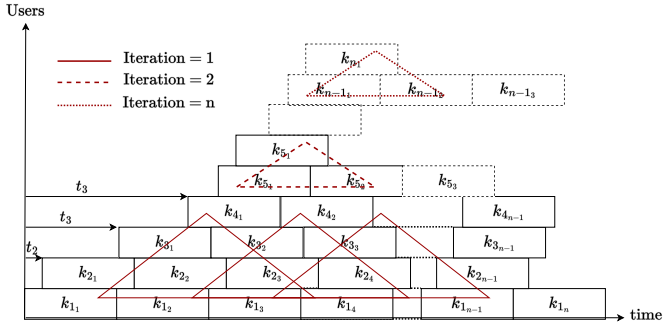

Figure 5: Proposed sequential T-SIC decoding scheme

Algorithm 1: Optimization algorithm: SIC triangle

Data: $SINR_k$, Δ_i of each k^{th} user
Result: Optimal D_u
Initialize m = 1, n = 1, $\lambda \succcurlyeq 0$
Set error tolerances for algorithm termination, ϵ_1, ϵ_2
repeat
  Initialize D_u
  repeat
    Run optimization problem in (9a)
    Update D_u as in (14)
    n = n+1
  until D_u *converged, i.e* $||\nabla_{D_u{}^{n-1}}|| \leq \epsilon_1$;
  Update λ as in (16)
  m = m+1
until λ *converged, i.e* $||\nabla_{\lambda^{m-1}}|| \leq \epsilon_2$;
Return D_u

In order to ensure that all K user data will be decoded, an algorithm called Cyclic T-SIC, is used to decode each users' data under multiple iterations, considering also the retransmissions by such users. Hence, the optimal set of data symbols will be decoded at the first iteration, based on the proposed optimization in (9a), and then R will repeat the process of listening to the same subcarrier and receiving the remaining users' data. Protocols utilized in outband D2D such as M-HELP [27] are designed such that the the transmitter UEs, whose data were not forwarded by neighbor devices, will re-transmit their own data after a fixed time interval using the same subcarrier over to the set of same neighbor nodes (R_n), $R \in R_n$. Such remaining user data transmitted to R will share the same subcarrier according to the protocol and will be superimposed such that it will be decoded using the optimization problem in (9a). Correspondingly, this method is repeated until all K user data are decoded using the proposed optimization-assisted SIC. To sum up, in Cyclic T-SIC, the decoding of user data will be done in multiple iterations, unlike the *Conv SIC* and T-SIC methods, taking into consideration maximum interference and minimum rate constraints.

Such Cyclic T-SIC algorithm at the receiver terminal is summarized in Algorithm 2. Further, the procedure followed at the transmitting UEs is given in Algorithm 4, where n_{RS}, n_{Rt} respectively gives the relaying count and re-transmissions count. Moreover, the proposed Cyclic T-SIC decoding in n iterations is as presented in Figure. 5. Furthermore, although recent studies have investigated the performance of the *Conv T-SIC* aided A-NOMA [9] in the uplink communications in terms of reliability, throughput, the performance analysis of a D2D A-NOMA scheme in terms of energy efficiency, reliability, computational complexity and delay aspects has been understudied.

V. Performance Analysis

In this section, the energy efficiency (EE), theoretical bit error rate (BER), computational complexity, and simulation delay of the proposed method are investigated.

Algorithm 2: At the receiver: sequential SIC decoding

Data: Total number of users sharing same resource, K
Initialize k_{opt} to 0
repeat
  Receive $n(\leq K)$ user data superimposed signal
  Derive the optimal D_u using (9a)
  Decoding the $k_{opt}(\leq n)$ user data
until *All* K *user data decoded*;

Algorithm 3: At the transmitters

Data: Relaying threshold, $RS_{\text{threshold}}$, retransmissions threshold, n_0
Initialize $n_{RS} = 0$, $n_{Rt} = 0$
repeat
  Listen to dedicated D2D emergency call channel
  re-transmitting in the same resource in next period
until $n_{RS} \geq RS_{threshold}$ *or* ,$n_{Rt} \geq n_0$;

A. Energy efficiency (EE) analysis:

Energy efficiency of the A-NOMA D2D scheme can be formulated as:

$$EE = \frac{R_{\text{total}}}{P_{\text{total}}} = \frac{\sum_{k=1}^{K} B.\log_2(1+SINR_k)}{\frac{1}{t_{ts}}E_c + P_{\text{circuit}}}, \tag{17}$$

where,

$$E_c = E_{\max} - E_{\max} e^{-\frac{ln(2)}{1000}\cdot\sum_{k=1}^{K} D_{u_k}\cdot k}, \tag{18}$$

the power consumption over single SIC iteration and P_{circuit} present the power dissipated by user device hardware circuits [18], [28], and $E_{\max}$, is the initial maximum energy in the user device.

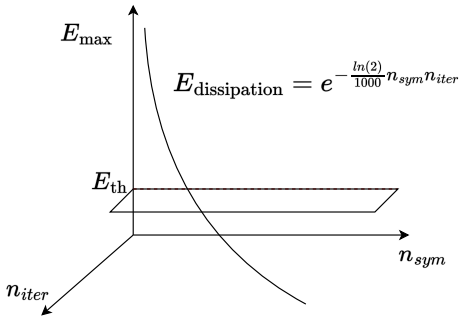

Figure 6: Energy dissipation curve for decoding n number of symbols

B. BER analysis:

The average theoretical BER of $k^{*^{th}}$ user data, P_{bit,k^*}, in asynchronous transmissions can be formulated as follows [9]. The error probability of s^{th} symbol detection can be presented with respect to the $(\tilde{\gamma}_k[s]|\mathbf{z}, h_{k^*}, \Delta_{k^*}[s])$ as,

$$P(e_{k^*}[s]|\mathbf{z}, h_{k^*}, \Delta_{k^*}[s]) = 1- \left(1 - Q\left(\sqrt{\frac{3.(\tilde{\gamma}_k[s]|\mathbf{z}, h_{k^*}, \Delta_{k^*}[s])}{2.(M-1)}}\right)\right)^2,$$

where, Q(·) represent the Q function.

$$(\tilde{\gamma}_k[s]|\mathbf{z}, h_{k^*}, \Delta_{k^*}[s]) = \text{Var}(\tilde{\eta}_k[s]|\mathbf{z}, \Delta_{k^*}[s]) + \sigma^2 > d_{e_k^*} \tag{19}$$

where $d_{e_k^*}$ is half the distance between two nearest constellation points given by $\sqrt{\frac{3.P_{k^*}h_{k^*}}{2.(M-1)}}$. Further, the conditional error probability of the s^{th} symbol detection is obtained as,

$$P(e_{k^*}[s]|h_{k^*}, \Delta_{k^*}[s]) = \sum_{i=1}^{2^{2(k_{opt}-1)}} P(e_{k^*}[s]|iP_{z(\mathcal{L})}, h_{k^*}, \Delta_{k^*}[s]) \times \prod_{k\in k_{opt}, \zeta\in(s-1,s+1), k\neq k^*} Pr_{i,k}^{(\mathcal{L})}[\zeta],$$

Here

$$P(e_{k^*}[s]) = \frac{1}{\tau_{max} - \tau_{min}} \times \int_{\tau_{min}}^{\tau_{max}} \int_0^{\infty} P(e_{k^*}[s]|h_{k^*}, \Delta_{k^*}[s]) \times e^{-h_{k^*}}.dh_{k^*}.d\Delta_{k^*}[s], \tag{20}$$

$$P_{bit,k^*} = \frac{P(e_{k^*}[s])}{\log_2(M)}, \tag{21}$$

where $P(e_{k^*}[s])$, $P(e_{k^*}[s]|\alpha_{k^*}, \Delta_{k^*}[s])$ denote respectively, the probability of error and conditional probability of error on the s^{th} symbol of the $k^{*^{th}}$ user. Also, s^{th} symbol of the k^* user is the desired symbol to be detected and M is the modulation order. Further, h_{k^*} denotes the magnitude of fading for the s^{th} symbol of the $k^{*^{th}}$ user. The $\Delta_{k^*}[s]$ denotes the percentage of symbol time that the overlapping symbols of the k^{th} user has on the s^{th} symbol of the $k^{*^{th}}$ user. Moreover, iP_z, denote probability of the i^{th} permutation of $\mathbf{z}$, $1 \leq i \leq 2^{2(k_{opt}-1)}$) and $Pr_{i,k}[\zeta]$ denote the probability of detection being correct or in error.

C. Computational Complexity analysis:

1) *Conv T-SIC:* The total interference to the desired symbol s^{th} symbol of k^{th} user, $\eta_k[s]$, is successively cancelled in conventional T-SIC process and hence the maximum computational complexity depends on the number of user devices, K, which is approximately of order $O(K^2)$ [18]..
2) *Cyclic T-SIC:* The decoding process of the proposed method has a complexity of $O(k_{opt}^2)$, where $k_{opt} \leq K$. On top of that the computational complexity for the stochastic gradient descent method based optimization in the proposed method is in the order of $O(log(\frac{1}{\epsilon}))$ [18]. To sum up, the proposed Cyclic T-SIC method has a computational complexity of $O(log(\frac{1}{\epsilon})k_{opt}^2)$ per single decoding iteration. Further, it is proven from **Lemma 1**, that the computational complexity is lesser in Cyclic T-SIC than the *Conv T-SIC*.

Table I: Simulation parameters

Parameter	**Value**
Modulation order, M	4 QAM
Minimum relative symbol time offset, τ_{min}	0.01 sec
Maximum relative symbol time offset , τ_{max}	0.5 sec
Maximum initial energy of user device, $E_{\max}$	10 V
power dissipated by user device, P_{circuit}	0.01 W
Maximum transmit power, $P_{\max}$	20 W
Path-loss exponent, η	1.5
Minimum throughput threshold, $R_{\min}$	2 Mbits/sec
Interference threshold, (I_{th})	1.2 mW
Interference minimum threshold, (I_{min})	0.01 mW
AWGN power, σ^2	0.01 W
Bandwidth, B	1 MHz
Symbol time duration, T_{sym}	1 sec
Maximum interference threshold, I_{th}	1.2 mW
Error tolerance for optimal D_u, ϵ_1	0.1
Error tolerance for optimal λ, ϵ_2	0.5
Learning rates, α and β	0.4
Transmission power of an UE	[0,...,$P_{\max}$]
Total number of UEs, K	[2,...25]
Symbol time offset between users	[1 - 50]%.T_{sym}
Energy saving priority, ϕ	[1,...,10]
Received power ratio, ν	[1,...,10]

Lemma 1. *The computational complexity of Cyclic T-SIC decoding of k_i user data over n iterations is less than that of conventional SIC decoding of K user data in one iteration [18]. Note that k_i is k_{opt} in the i^{th} iteration and the sum of k_i equals K.*

$$\log\left(\frac{1}{\epsilon}\right)\sum_{i=1}^{n} k_i^2 \leq K^2, \tag{22}$$

where, $0.1 < \epsilon < 1$, $k_i \leq K$ *and* $\sum_{i=1}^{n} k_i = K$

Proof. Consider

$$K = k_1 + k_2 + k_3 + ... + k_i + ... + k_{n-1} + k_n \tag{23}$$

where $k_i \leq K$. Hence,

$$k_i^2 \leq K^2 \tag{24}$$

Further, it can be seen that,

$$\sum_{i=1}^{n} k_i^2 \leq \left(\sum_{i=1}^{n} k_i\right)^2 = \sum_{i=1}^{n} k_i^2 \leq K^2. \tag{25}$$

Moreover,

$$\log\left(\frac{1}{\epsilon}\right)\sum_{i=1}^{n} k_i^2 \leq K^2 \tag{26}$$

where $0.1 < \epsilon < 1$. □

VI. Result analysis

In this Section, the numerical results to demonstrate the significance of the proposed algorithm in terms of EE are presented. All terminals were considered to be randomly located within a radius of 100 m to the corresponding receiving UE and all the results were averaged over 100 various random locations of UEs. The parameters used in our simulation are summarized in Table. I. It should be noted that these parameters can be modified to any other values depending on the specific scenario under consideration.

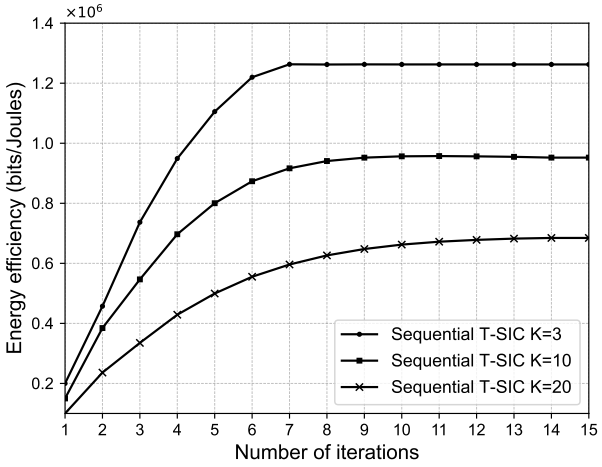

Figure 7: Convergence in Energy efficiency of the proposed Cyclic T-SIC system under varying number of users. Parameters: ν = 5, interference threshold (I_{th}) = 1.2 mW, relative symbol time offset = 0.15%.

A. Convergence

In the first simulation, the convergence performance of the proposed Cyclic T-SIC algorithm was studied. As shown in Figure. 7, it was observed that the EE obtained, based on the proposed optimization algorithm, converges to a stable value (optimal EE) within a fixed number of iterations, even if the number of users K incremented.

B. EE performance

In the proceeding simulation, the EE performance of the proposed algorithm with varying number of users was studied and compared with the *Conv T-SIC*. From Figure. 8, it was seen that the EE decreased with the number of users. Indeed, with the increment in the number of users, the number of computations increases which results in a higher energy consumption and thus a lesser EE. Also, the gradient of EE decline was higher initially, since the k_{opt} to be decoded per iteration is lower when the difference between K and k_{opt} is lesser when compared to the proceeding cases where the K is higher. Moreover, with the increase in the interference threshold, the energy efficiency reduced because the number of users selected to be decoded incremented due to the increase in the maximum interference limit. Since *Conv T-SIC* is not optimizing the number of users, it is not impacted by such an interference threshold constraint. In *Conv T-SIC*, the maximum number of received data are decoded each time which leads to higher energy consumption compared to Cyclic T-SIC. Hence, an EE gain of 35.66% by Cyclic T-SIC over *Conv T-SIC* was observed in this scenario. Moreover, the EE saturated after the number of users reached a specific limit. Once the fixed limiting thresholds in the optimization constraints are satisfied, the k_{opt} data decoded per iteration in Cyclic T-SIC reaches a specific limit. Further, the instance where such EE convergence occurs can vary upon the simulation parameters used.

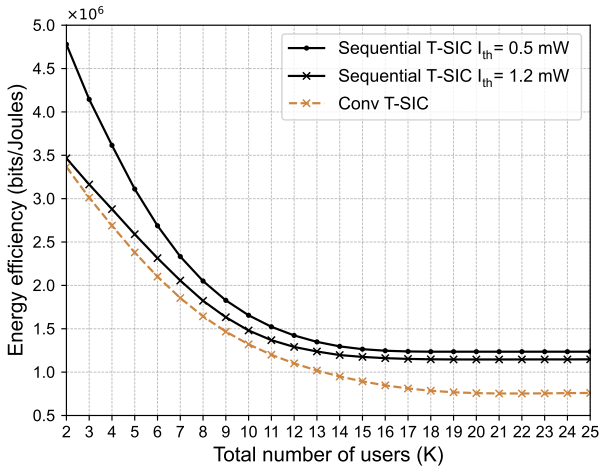

Figure 8: Energy efficiency (EE) vs total number of users under varying interference threshold constraints. Parameters: received power ratio, ν = 5, relative symbol time offset = 0.15%.

In the next simulation, the variation of EE against the received power ratio, ν, was observed. As seen in the Figure. 9, EE incremented with the increase in ν for both Cyclic and Conv T-SIC since the sum throughput incremented with the ν. Further, Cyclic T-SIC has a significant improvement in comparison to Conv T-SIC, because the increment in ν enables the optimization algorithm to easily compute the k_{opt} due to the difference in each user data signal power levels. Hence, the efficiency of decoding increases per each iteration. Further, with the increment in the number of users, the EE has decreased since the number of user data decoded increases. Further, it was noted that Cyclic T-SIC had an EE gain by 79.86% compared to Conv T-SIC. Also, a convergence in EE was observed after a specific ν. This was caused due to the limiting thresholds in the optimization algorithm which constrained the k_{opt} decoded.

In the proceeding simulation, the variation of EE against the number of users in the same subcarrier was studied. The EE incremented swiftly for a certain range of users and decreased gradually thereafter since the energy dissipation became significant compared to the throughput at the receiver. The initial increment in EE value of the proposed Cyclic T-SIC

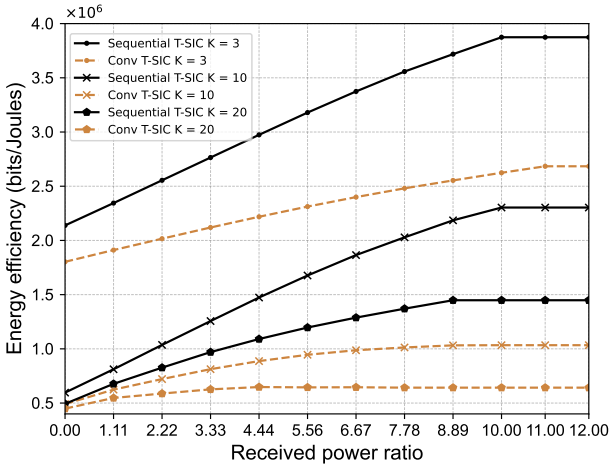

Figure 9: Energy efficiency vs received power ratio (ν) under varying number of users. Parameters: interference threshold (I_{th}) = 1.2 mW, relative symbol time offset = 0.15%.

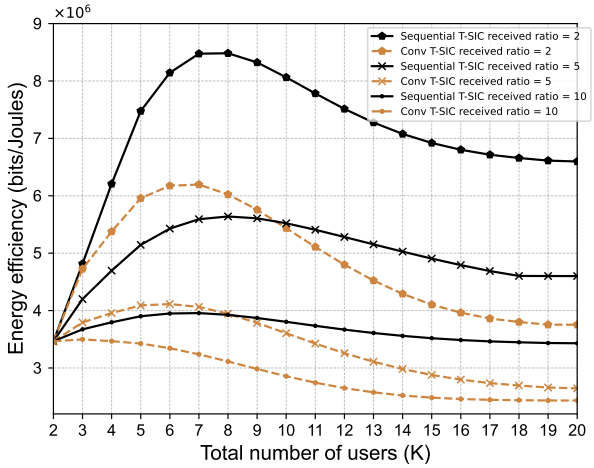

Figure 10: Energy efficiency vs total number of users under varying received power ratio (ν). Parameters: interference threshold (I_{th}) = 1.2 mW, relative symbol time offset = 0.15 %, transmit SNR = 60 dB.

is due to the optimization of users suitably, under the constraint thresholds, even when the number of users increase. Hence, as seen in Figure. 10, the EE increased and reached a maximum but declined after a such point because of the increment in the decoded user symbols since the optimization maximizes the decoded symbols under the statistical interference threshold and rate constraints. Further, under different νs, an increment in the EE of the *Conv T-SIC* was observed because with the increase in ν, the difference in user data signal power levels becomes significant. The optimization algorithm is designed to choose the optimal amount of users that minimizes energy dissipation. Next, the EE was observed to decline with the number of users, since number of symbols to be decoded increases with the number of users and with that the energy consumption increases. Finally, the EE value starts converging, since the number of users decoded reaches a limit under constraint imposed by the proposed optimization problem. In addition, an EE gain by 40.16% was observed in this scenario compared to Conv T-SIC.

C. BER performance

In the following simulation, the theoretical bit error rate (BER_{th}) of the proposed Cyclic T-SIC was studied with the *Conv T-SIC*. As seen in Figure. 11a, the average BER_{th} performance in the proposed method was seen to be improved than *Conv T-SIC*. The proposed Cyclic T-SIC method optimizes the k_{opt} per iteration and decodes all K users over successive receptions compared to decoding all received data in a single iteration. Moreover, a BER reduction of 38.33% by Cyclic T-SIC over Conv T-SIC was observed in this scenario.

D. Trade-off between EE and BER

In the next simulation, the BER of each individual user data was studied against the ν. As seen in the Figure 11b, the proposed scheme has an improved BER for the the nearest, middle, and farthest users, compared to *Conv T-SIC*. The optimization algorithm impacts the selection of user data to be decoded depending on the power level and interference level on each data. Hence, consideration of such factors lead into selecting the optimal k_{opt} per SIC decoding iteration in Cyclic T-SIC method. Moreover, the trade-off between EE and BER curves under Cyclic T-SIC was observed. It was seen that the proposed scheme can achieve a higher energy efficiency and reduced BER than *Conv T-SIC* under a lower ν. Furthermore, a BER reduction of 46.77% by Cyclic T-SIC over Conv T-SIC was observed in this case.

Further, in the proceeding simulation, the EE and BER performance of the proposed scheme was compared with the *Conv T-SIC* against transmit SNR and presented in Figure. 12. The proposed system had an improved BER because of selecting the optimal user signals to be decoded based on the divergence of power levels of each user signal. Further, for BER reduced with the increment in transmit SNR because the SIC decoding enhanced with the divergent power levels. Moreover, the EE of the proposed system was higher than *Conv T-SIC*, because it optimally selected the number of user data decoded per iteration and reduced the overall energy consumption. The intersection point of BER and EE curves of Cyclic T-SIC method was achieved at a lower transmit SNR than the *Conv T-SIC* method. Hence, with lower transmit SNR, a higher EE and reduced BER can be gained using Cyclic T-SIC compared to *Conv T-SIC*. It was observed that the proposed scheme has enhanced EE by 95% and reduced average BER by 61% with respect to the transmit SNR.

Moreover, the EE and BER performance of the proposed scheme was compared with the *Conv T-SIC* against the relative symbol time offset between users in Figure. 13. BER performance worsened with the increment in symbol time

offset. However, the proposed system had an improved BER because of considering the optimal user data to be decoded at each iteration depending on the interference added by relative symbol time offsets. Moreover, the EE of the proposed system was higher than *Conv T-SIC*, although the interference between users increased with the symbol time offset. The optimization of number of user data decoded based on the interference threshold, limits the number of users decoded per iteration, which result in improving BER and EE of the proposed Cyclic T-SIC. Further, the intersection points of nearest user BER and EE was achieved at a relative symbol time-offsets of 0.04%. At such a point, when the time-offset was 0.04%, a higher EE and lower BER was obtained by Cyclic T-SIC than *Conv T-SIC*. Hence, a lower BER and higher EE can be obtained even if the time-offset increases the asynchrony among the received data signals in the proposed Cyclic T-SIC scheme. The EE and BER had an improvement respectively, by 92.3% and 94.7%.

E. Complexity and delay analysis

In the next simulation, the theoretical computational complexity of the proposed method was compared with the *Conv T-SIC*. The curve with the proposed Cyclic T-SIC has a considerably lower complexity order compared to the *Conv T-SIC* as seen in Figure. 14a. In Cyclic T-SIC, the user data decoding happens in a sequential manner, by optimization of k_{opt} data that can be decoded per each iteration. Moreover, a complexity reduction of 56.14% by Cyclic T-SIC over Conv T-SIC was observed in this case.

In the last simulation, the total simulation delay against the number of users, K, was compared between the Cyclic T-SIC and the *Conv T-SIC* methods as shown in Figure 14b. It was observed that the average simulation delay in Cyclic T-SIC is lower than that of *Conv T-SIC* to decode all K user data. As K increases, the decoding delay increases in Conv T-SIC decoding. In contrast, in Cyclic T-SIC, since k_{opt} data per iteration is, on average, lower than K, the delay per iteration becomes less. Further, the delay decreases as the k_{opt} data decoded per each successive iteration decreases. Also, a simulation delay reduction of 22.44% by Cyclic T-SIC over Conv T-SIC was observed in this case.

VII. Conclusion

In this paper, we have addressed the decoding efficiency problem in an A-NOMA enabled D2D network. Our goal was to select the optimal combination of the user data symbols to decoded while satisfying the constraints in terms of maximum statistical interference threshold, and minimum rate. The corresponding optimization problem was a hard constraint problem due to binary optimization variables and non linear constraints, and thus the solution cannot be derived directly. In order to obtain a feasible solution, the binary variables were relaxed and a Lagrangian dual algorithm based on convex programming was proposed. Numerical results demonstrate the BER and EE performance of the proposed system under varying parameters such as interference constraints, number of user data, received power ratio, transmit SNR, etc. On average, the proposed Cyclic T-SIC method had EE gains by 74.73% and BER reductions by 36.78% compared to Conv T-SIC . Further, computational complexity and simulation delay of the proposed Cyclic T-SIC was below Conv T-SIC respectively by 56.14% and 22.44%.

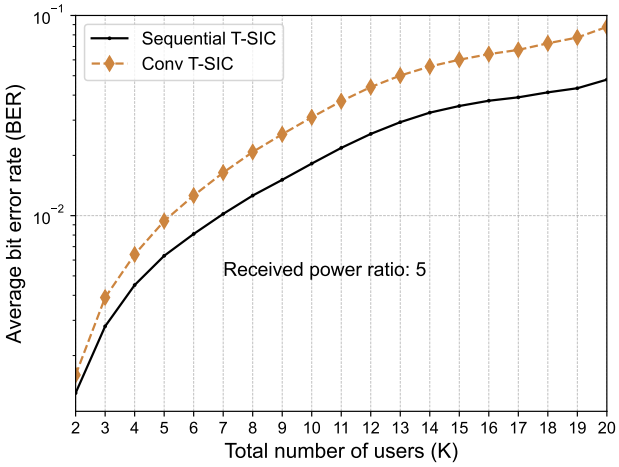

(a) BER of the nearest user vs number of users (K). Parameters: received power ratio, ν = 5, interference threshold (I_{th}) = 1.2 mW, relative symbol time offset = 0.15.

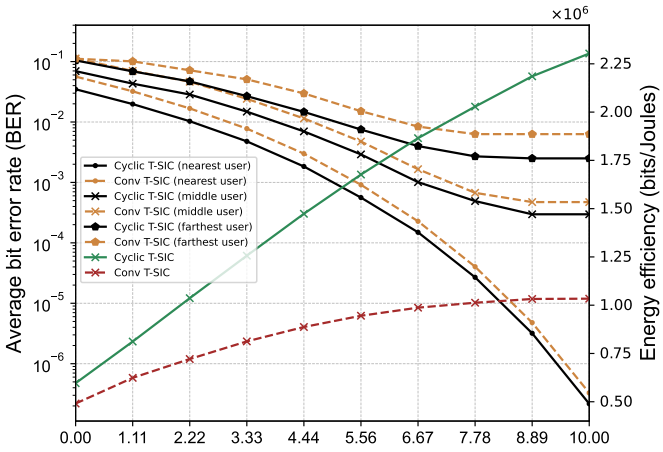

(b) BER vs received power ratio (ν)

Figure 11: BER analysis of the proposed Cyclic T-SIC. Parameters: interference threshold (I_{th}) = 1.2 mW, received power ratio, ν = 5, number of users = 10

References

[1] V. Basnayake, D. N. K. Jayakody, V. Sharma, N. Sharma, P. Muthuchidambaranathan, and H. Mabed, "A new green prospective of non-orthogonal multiple access (noma) for 5g," *Information*, vol. 11, no. 2, 2020. [Online]. Available: https://www.mdpi.com/2078-2489/11/2/89

[2] M. Agiwal, H. Kwon, S. Park, and H. Jin, "A survey on 4g-5g dual connectivity: Road to 5g implementation," *IEEE Access*, vol. 9, pp. 16 193–16 210, 2021.

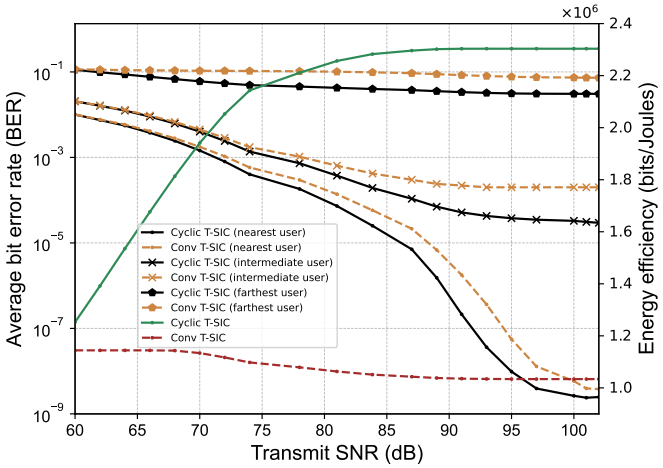

Figure 12: EE and BER vs transmit SNR. Parameters: interference threshold (I_{th}) = 1.2 mW, received power ratio, ν = 5, number of users = 10, relative symbol time offset = 0.15%.

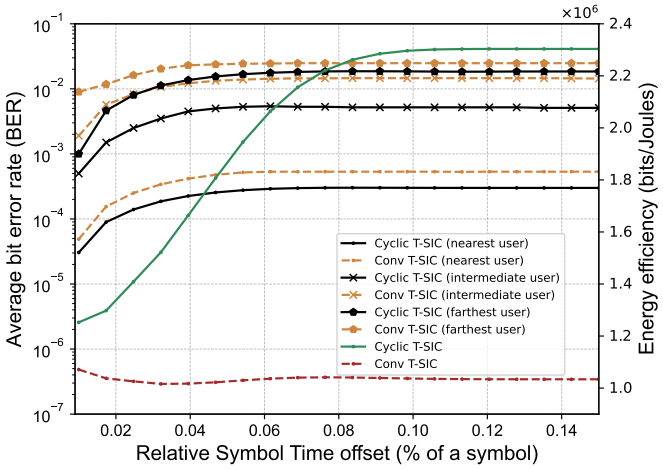

Figure 13: EE and BER vs time-offset. Parameters: interference threshold (I_{th}) = 1.2 mW, received power ratio, ν = 5, number of users = 10

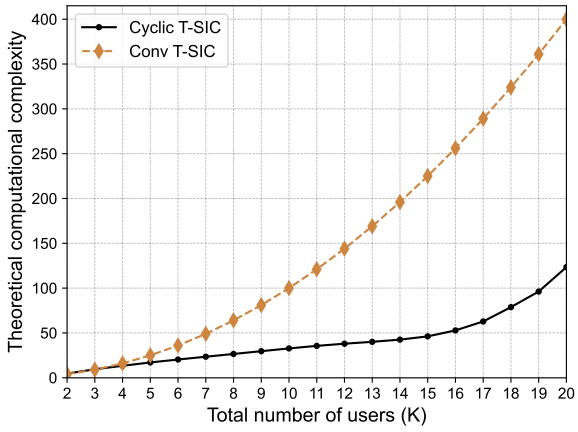

(a) Computational complexity vs total number of users (K). Parameters: interference threshold (I_{th}) = 1.2 mW, received power ratio, ν = 5, relative symbol time offset = 0.15%.

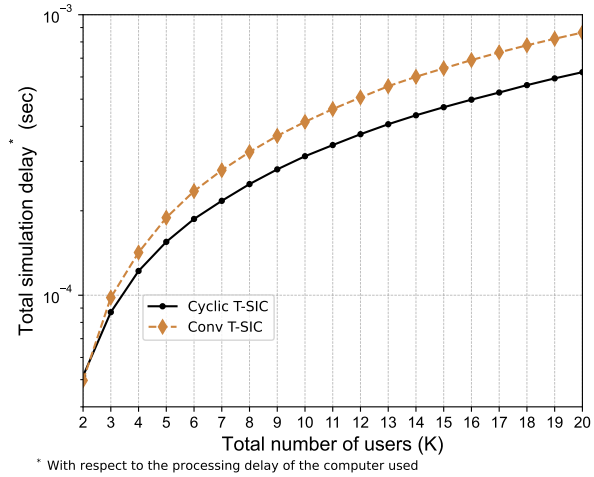

(b) Total simulation delay vs total number of users (K). Parameters: interference threshold (I_{th}) = 1.2 mW, received power ratio, ν = 5, relative symbol time offset = 0.15%.

Figure 14: Computational complexity and simulation delay of proposed Cyclic T-SIC.

[3] H. I. Fitriasari, A. I. Lestari, D. L. Luhurkinanti, and R. F. Sari, "Performance evaluation of downlink multi-user ofdma scheduling in 5g new radio (nr)," in *2021 18th International Conference on Electrical Engineering/Electronics, Computer, Telecommunications and Information Technology (ECTI-CON)*, 2021, pp. 219–223.

[4] D. Thiyagarajan and P. Venkatesan, "Performance estimation of multi-carrier cdma using adaptive brain storm optimization for 5g communication system in frequency selective fading channel," 12 2019.

[5] Y. Liu, W. Yi, Z. Ding, X. Liu, O. A. Dobre, and N. Al-Dhahir, "Developing noma to next generation multiple access (ngma): Future vision and research opportunities," *IEEE Wireless Communications*, pp. 1–8, 2022.

[6] Z. Ding, R. Schober, and H. V. Poor, "Unveiling the importance of sic in noma systems—part 1: State of the art and recent findings," *IEEE Communications Letters*, vol. 24, no. 11, pp. 2373–2377, 2020.

[7] S. Gamboa, F. J. Cintron, D. Griffith, and R. Rouil, "Adaptive synchronization reference selection for out-of-coverage proximity services," in *2017 IEEE 28th Annual International Symposium on Personal, Indoor, and Mobile Radio Communications (PIMRC)*, 2017, pp. 1–7.

[8] C. Liu and N. C. Beaulieu, "Exact ber performance for symbol-asynchronous two-user non-orthogonal multiple access," *IEEE Communications Letters*, vol. 25, no. 3, pp. 764–768, 2021.

[9] H. Haci, H. Zhu, and J. Wang, "Performance of non-orthogonal multiple access with a novel asynchronous interference cancellation technique," *IEEE Transactions on Communications*, vol. 65, no. 3, pp. 1319–1335, 2017.

[10] F. Lu, M. Xu, L. Cheng, J. Wang, and G.-K. Chang, "Power-division non-orthogonal multiple access (noma) in flexible optical access with synchronized downlink/asynchronous uplink," *Journal of Lightwave Technology*, vol. 35, no. 19, pp. 4145–4152, 2017.

[11] X. Wang, F. Labeau, and L. Mei, "Asynchronous uplink non-orthogonal multiple access (noma) with cyclic prefix," in *2018 IEEE Wireless Communications and Networking Conference (WCNC)*, 2018, pp. 1–6.

[12] X. Zou, B. He, and H. Jafarkhani, "An analysis of two-user uplink asynchronous non-orthogonal multiple access systems," *IEEE Transactions on Wireless Communications*, vol. 18, no. 2, pp. 1404–1418, 2019.

[13] ——, "On uplink asynchronous non-orthogonal multiple access systems with timing error," in *2018 IEEE International Conference on Commu-*

nications (ICC), 2018, pp. 1–6.

[14] J. Liu, Y. Li, G. Song, and Y. Sun, "Detection and analysis of symbol-asynchronous uplink noma with equal transmission power," *IEEE Wireless Communications Letters*, vol. 8, no. 4, pp. 1069–1072, 2019.

[15] X. Zou, M. Ganji, and H. Jafarkhani, "Cooperative asynchronous non-orthogonal multiple access with power minimization under qos constraints," *IEEE Transactions on Wireless Communications*, vol. 19, no. 3, pp. 1503–1518, 2020.

[16] M. Ganji, X. Zou, and H. Jafarkhani, "Asynchronous transmission for multiple access channels: Rate-region analysis and system design for uplink noma," *IEEE Transactions on Wireless Communications*, vol. 20, no. 7, pp. 4364–4378, 2021.

[17] W. U. Khan, M. A. Javed, T. Nguyen, S. Khan, and B. ElHalawany, "Energy-efficient resource allocation for 6g backscatter-enabled noma iov networks," *IEEE Transactions on Intelligent Transportation Systems*, vol. PP, pp. 1–11, 09 2021.

[18] J. Tang, J. Luo, M. Liu, D. So, E. Alsusa, G. Chen, K.-K. Wong, and J. Chambers, "Energy efficiency optimization for noma with swipt," *IEEE Journal of Selected Topics in Signal Processing*, vol. PP, pp. 1–1, 02 2019.

[19] U. Samaratunge, D. N. Jayakody, S. Biswash, and R. Dinis, "Recent advances and future research challenges in non-orthogonal multiple access for 5g networks," 05 2018.

[20] R. Shankar, "Examination of a non-orthogonal multiple access scheme for next generation wireless networks," *The Journal of Defense Modeling and Simulation*, vol. 19, no. 3, pp. 453–465, 2022.

[21] A. Zafar, M. Shaqfeh, M.-S. Alouini, and H. Alnuweiri, "On multiple users scheduling using superposition coding over rayleigh fading channels," *Communications Letters, IEEE*, vol. 17, pp. 733–736, 04 2013.

[22] H. Baek, W. J. Yun, S. Jung, J. Park, M. Ji, J. Kim, and M. Bennis, "Communication and energy efficient slimmable federated learning via superposition coding and successive decoding," *CoRR*, vol. abs/2112.03267, 2021. [Online]. Available: https://arxiv.org/abs/2112.03267

[23] X. Chen, L. Pu, L. Gao, W. Wu, and D. Wu, "Exploiting massive d2d collaboration for energy-efficient mobile edge computing," *IEEE Wireless Communications*, vol. 24, no. 4, pp. 64–71, 2017.

[24] E. Che, H. D. Tuan, and H. H. Nguyen, "Joint optimization of cooperative beamforming and relay assignment in multi-user wireless relay networks," *IEEE Transactions on Wireless Communications*, vol. 13, no. 10, pp. 5481–5495, 2014.

[25] S. He, J. Yuan, Z. An, W. Huang, Y. Huang, and Y. Zhang, "Joint user scheduling and beamforming design for multiuser miso downlink systems," 2021. [Online]. Available: https://arxiv.org/abs/2112.01738

[26] X. Wang, L. Yan, and Q. Zhang, "Research on the application of gradient descent algorithm in machine learning," in *2021 International Conference on Computer Network, Electronic and Automation (ICCNEA)*, 2021, pp. 11–15.

[27] V. Basnayake, H. Mabed, D. N. K. Jayakody, and P. Canalda, "M-help - multi-hop emergency call protocol in 5g," in *2020 IEEE 19th International Symposium on Network Computing and Applications (NCA)*, 2020, pp. 1–8.

[28] E. Björnson, M. Kountouris, and m. Debbah, "Massive mimo and small cells: Improving energy efficiency by optimal soft-cell coordination," 04 2013.